2022 SCRP Fisher Lab Application Assignment

Prof. Fisher's research project this summer centers on the recombinant expression, purification, and characterization of a putative halide methyltransferase enzyme from the moss *Physcomitrela patens*. If you are interested in applying to work with her, please read the article by Nagatoshi and Nakamura in the Journal of Biological Chemistry and schedule an appointment with Prof. Fisher to discuss the article with her.

To schedule an appointment with Prof. Fisher, please email her at ajfisher@willamette.edu.

Enzyme Catalysis and Regulation:
Arabidopsis* HARMLESS TO OZONE LAYER Protein Methylates a Glucosinolate Breakdown Product and Functions in Resistance to *Pseudomonas syringae* pv. *maculicola

Yukari Nagatoshi and Tatsuo Nakamura
J. Biol. Chem. 2009, 284:19301-19309.
doi: 10.1074/jbc.M109.001032 originally published online May 6, 2009

Access the most updated version of this article at doi: 10.1074/jbc.M109.001032

Find articles, minireviews, Reflections and Classics on similar topics on the JBC Affinity Sites.

Alerts:
- When this article is cited
- When a correction for this article is posted

Click here to choose from all of JBC's e-mail alerts

Supplemental material:
http://www.jbc.org/content/suppl/2009/05/06/M109.001032.DC1.html

This article cites 43 references, 16 of which can be accessed free at
http://www.jbc.org/content/284/29/19301.full.html#ref-list-1

Downloaded from http://www.jbc.org/ at WILLAMETTE UNIVERSITY on August 29, 2014

THE JOURNAL OF BIOLOGICAL CHEMISTRY VOL. 284, NO. 29, pp. 19301–19309, July 17, 2009
© 2009 by The American Society for Biochemistry and Molecular Biology, Inc. Printed in the U.S.A.

Arabidopsis HARMLESS TO OZONE LAYER Protein Methylates a Glucosinolate Breakdown Product and Functions in Resistance to *Pseudomonas syringae* pv. *maculicola*[*][S]

Received for publication, March 31, 2009 Published, JBC Papers in Press, May 6, 2009, DOI 10.1074/jbc.M109.001032

Yukari Nagatoshi and Tatsuo Nakamura[1]

From the Graduate School of Environment and Information Sciences, Yokohama National University, Yokohama, Kanagawa 240-8501, Japan

Almost all of the chlorine-containing gas emitted from natural sources is methyl chloride (CH_3Cl), which contributes to the destruction of the stratospheric ozone layer. Tropical and subtropical plants emit substantial amounts of CH_3Cl. A gene involved in CH_3Cl emission from *Arabidopsis* was previously identified and designated *HARMLESS TO OZONE LAYER* (hereafter *AtHOL1*) based on the mutant phenotype. Our previous studies demonstrated that AtHOL1 and its homologs, AtHOL2 and AtHOL3, have *S*-adenosyl-L-methionine-dependent methyltransferase activities. However, the physiological functions of AtHOLs have yet to be elucidated. In the present study, our comparative kinetic analyses with possible physiological substrates indicated that all of the AtHOLs have low activities toward chloride. AtHOL1 was highly reactive to thiocyanate (NCS^-), a pseudohalide, synthesizing methylthiocyanate (CH_3SCN) with a very high k_{cat}/K_m value. We demonstrated *in vivo* that substantial amounts of NCS^- were synthesized upon tissue damage in *Arabidopsis* and that NCS^- was largely derived from myrosinase-mediated hydrolysis of glucosinolates. Analyses with the T-DNA insertion *Arabidopsis* mutants (*hol1*, *hol2*, and *hol3*) revealed that only *hol1* showed increased sensitivity to NCS^- in medium and a concomitant lack of CH_3SCN synthesis upon tissue damage. Bacterial growth assays indicated that the conversion of NCS^- into CH_3SCN dramatically increased antibacterial activities against *Arabidopsis* pathogens that normally invade the wound site. Furthermore, *hol1* seedlings showed an increased susceptibility toward an *Arabidopsis* pathogen, *Pseudomonas syringae* pv. *maculicola*. Here we propose that AtHOL1 is involved in glucosinolate metabolism and defense against phytopathogens. Moreover, CH_3Cl synthesized by AtHOL1 could be considered a byproduct of NCS^- metabolism.

Methyl chloride (CH_3Cl) is the most abundant halohydrocarbon emitted into the atmosphere and constitutes about 17% of the chlorine currently in the stratosphere (1). CH_3Cl is derived mainly from natural sources and contributes to the destruction of the stratospheric ozone layer. As the total abundance of ozone-depleting gases such as chlorofluorocarbons in the atmosphere has begun to decrease in recent years as a result of The Montreal Protocol on Substances That Deplete the Ozone Layer, the impact of CH_3Cl emission from natural sources will become greater on the atmospheric chemistry. CH_3Cl emission into the atmosphere has been estimated at 1,700–13,600 Gg/year (1), which underscores the great uncertainty of the estimation. Oceans (2), biomass burning (3), wood-rotting fungi, and coastal salt marshes (4) are the major sources of CH_3Cl production. Recently, it was reported that large amounts of CH_3Cl are emitted from tropical and subtropical plants, which are hence considered as the major sources of CH_3Cl (5–7). It was estimated that the CH_3Cl emission from tropical plants could account for 30–50% of the global CH_3Cl emission (8). To accomplish an accurate estimation of CH_3Cl production in the atmosphere through "bottom-up" approaches, elucidating the mechanisms and physiological functions of CH_3Cl emission from plants will be important.

The biological synthesis of methyl halides has been demonstrated mainly by biochemical analyses. The enzymatic activities that transfer a methyl group from *S*-adenosyl-L-methionine (SAM)[2] to halide ions (Cl^-, Br^-, I^-), which synthesize methyl halides, were first discovered in cell-free extracts of *Phellinus pomaceus* (a white rot fungus), *Endocladia muricata* (a marine red alga), and *Mesembryanthemum crystallinum* (ice plant, a halophytic plant) (9). Enzyme purification and cDNA cloning of the methyl chloride transferase (MCT) was first reported with *Batis maritima*, a halophytic plant that grows abundantly in salt marshes. As high concentrations of ions such as Cl^- are often detrimental to plants, halophytic plants are considered to possess various salt tolerance mechanisms. MCT was hypothesized to control and regulate the internal concentration of Cl^-, rich in the habitat in which halophytic plant grows (10, 11).

In the meantime, purification of thiol methyltransferase (TMT), which methylates bisulfide (HS^-) and halide (Cl^-, Br^-, I^-) ions was reported with cabbage, *Brassica oleracea* (12). The purified and recombinant TMTs were later shown to also

* This work was supported by Grant-in-aid for Scientific Research 19780249 from the Ministry of Education, Science, Sports, and Culture of Japan (to T. N.), a Sasagawa Scientific Research Grant from the Japan Science Society (to Y. N.), and a research grant from the ESPEC Foundation for Global Environmental Research and Technology (to T. N.).

[S] The on-line version of this article (available at http://www.jbc.org) contains supplemental Table 1 and Figs. S1–S4.

[1] To whom correspondence should be addressed: 79-7 Tokiwadai, Hodogaya-ku, Yokohama, Kanagawa 240-8501, Japan. Fax: 81-45-339-4416; E-mail: t-nakamu@ynu.ac.jp.

[2] The abbreviations used are: SAM, S-adenosyl-L-methionine; GC-ECD, gas chromatography equipped with an electron capture detector; GC-MS, gas chromatography/mass spectrometry; HOL, harmless to ozone layer; HPLC, high performance liquid chromatography; MCT, methyl chloride transferase; MS, Murashige-Skoog; RT, reverse transcription; SAH, *S*-adenosyl-L-homocysteine; TMT, thiol methyltransferase.

Downloaded from http://www.jbc.org/ at WILLAMETTE UNIVERSITY on August 29, 2014

methylate the thiocyanate ion (NCS^-), which is called pseudohalide because of its chemical properties similar to halide ions (13, 14). NCS^- is a hydrolysis product found in some glucosinolates, which are secondary metabolites found mainly in the order Brassicales including the model plant *Arabidopsis thaliana* (15). Upon tissue damage such as by insect or herbivore attack, glucosinolates are hydrolyzed by myrosinase (β-thioglucosidase) into biologically active compounds including isothiocyanates. Isothiocyanates derived from indole glucosinolates and 4-hydroxybenzyl glucosinolates are reported to be highly unstable and yield NCS^- upon reacting with various nucleophiles (15–17). Based on the enzymatic activity, the physiological role of TMT was speculated to metabolize glucosinolate breakdown products (14). However, there are no reported studies that examine these MCT and TMT hypotheses through *in vivo* experiments.

An *Arabidopsis* homolog of MCT was also identified, and its T-DNA insertion *Arabidopsis* mutants were analyzed (18). Because the gene disruption eliminated almost all of the methyl halide emissions from the mutants, the gene was revealed to be involved in methyl halide synthesis and was designated *HOL* (*HARMLESS TO OZONE LAYER*; denoted as *AtHOL1* in our studies) based on the mutant phenotype (18). Recently, we identified *AtHOL1* homologs *AtHOL2* and *AtHOL3* in *Arabidopsis*, and we demonstrated biochemically that the three recombinant AtHOLs have SAM-dependent methyltransferase activities (19). In this study, reverse genetic and biochemical analyses of all AtHOL isoforms revealed that AtHOL1 *in vivo* is involved in the methylation of NCS^- produced by glucosinolate hydrolysis. Although there are several studies that have examined the biological activities of glucosinolate hydrolysis products, the mechanisms of NCS^- synthesis and its methylation to methyl thiocyanate (CH_3SCN) have yet to be reported in detail. The biological activity and physiological function of CH_3SCN synthesized by AtHOL1 was also examined.

EXPERIMENTAL PROCEDURES

Plant Materials and Growth Conditions—Wild-type *Arabidopsis* (*A. thaliana* ecotype Col-0), three T-DNA insertion *Arabidopsis* mutants (*hol1*, *hol2*, *hol3*), and the three *AtHOL1*-overexpressing *Arabidopsis* lines were used in this study. Seeds were sterilized and grown on half-strength Murashige-Skoog (MS) agar medium or soil under controlled conditions (12 h light/12 h dark cycle at 22 ± 1 °C).

Isolation of T-DNA Insertion Arabidopsis Mutants—T-DNA insertion *Arabidopsis* mutants (stock names *AtHOL1*, SALK_005204C; *AtHOL2*, SALK_021226C; *AtHOL3*, SALK_014648C) were obtained from the Nottingham Arabidopsis Stock Centre. Homozygous mutant plants were screened by two sets of PCR using genomic DNA as templates. In the first PCR, T-DNA insertion was confirmed using a T-DNA left border primer (LBb1) and a gene-specific primer (AtHOL1-2, AtHOL2-3, or AtHOL3-2). In the second PCR, homozygosity of the T-DNA insertions was determined using gene-specific primers (AtHOL1-2 and AtHOL1-3; AtHOL2-2 and AtHOL2-3; AtHOL3-2 and AtHOL3-3) (supplemental Table 1) that flank the inserted T-DNAs. mRNA accumulation in the screened homozygous mutant plants was examined by RT-PCR using gene-specific primer sets (AtHOL1-2 and AtHOL1/2-1; AtHOL2-8 and AtHOL2-9; AtHOL3-2 and AtHOL3-3). *AtPP2AA3* (At1g13320) was amplified with primers AtPP2AA3-1 and AtPP2AA3-2 as an internal control (20). Total RNA was purified from 4-week-old mutant plants, and cDNA was synthesized by Moloney murine leukemia virus reverse transcriptase (Promega, Madison, WI) using a poly(A) primer, attB2T19VN. RT-PCR conditions were as follows: denaturation at 98 °C for 2 min and then 35 cycles of 94 °C for 15 s, 55 °C for 30 s, and 72 °C for 50 s.

Phylogenetic Analysis—The amino acid sequences of HOL homologs deduced from the completed genomic sequences, cDNA sequences, and assembled expressed sequence tag sequences from various photosynthetic organisms were extracted through BLAST search (blast.ncbi.nlm.nih.gov/Blast.cgi) of the available nucleic acid sequence data bases. The unrooted phylogenetic tree was constructed based on the obtained amino acid sequences using the ClustalW (21) and Njplot programs (22).

Overexpression of AtHOL1 in Arabidopsis—The *AtHOL1* cDNA fragment containing the open reading frame was prepared by PCR (19) and cloned between the XbaI and XhoI sites in the binary vector pBI121 under the control of the cauliflower mosaic virus 35S promoter. The constructed binary vector (pBI121-AtHOL1) was introduced into *Agrobacterium tumefaciens* (LBA4404) by electroporation, which was then used to transform wild-type *Arabidopsis* by floral dipping. Transgenic T1 *Arabidopsis* were selected on half-strength MS agar medium containing 25 mg/liter kanamycin sulfate.

High Performance Liquid Chromatography (HPLC) Analyses—SAM-dependent methyltransferase activities were analyzed by ion pair reverse-phase HPLC using a Waters system (600 pump, 600E system controller, 486 tunable absorbance detector; Waters, Milford, MA). Samples were separated by the octadecylsilyl (ODS) column (4.6 × 150-mm; ODS-80Ts, Tosoh, Tokyo) protected by a guard column (ODS-80Ts guardgel, Tosoh) with 70% solvent A (8 mM octanesulfonic acid sodium salt, 50 mM NaH_2PO_4, pH 3.0 adjusted by H_3PO_4) and 30% solvent B (100% methanol) at an isocratic flow rate of 1.0 ml/min. *S*-adenosyl-L-homocysteine (SAH) was detected by UV absorption at 254 nm. The SAH was identified by comparison with the retention time of pure SAH.

GC-ECD and GC-MS Analyses—The quantitative determination of CH_3SCN was carried out by gas chromatography equipped with an electron capture detector (GC-ECD; GC-9A, Shimadzu, Kyoto, Japan). The samples in 2.0-ml glass vials were incubated at 70 °C for 30 min, and each headspace was sampled using a gas-tight syringe followed by an injection into a 200 × 0.3-cm inner diameter stainless column packed with Porapak Q (Waters) in the GC-ECD. The column and injection port temperatures were 180 and 250 °C, respectively, and the flow rate of the carrier gas (N_2) was 40 ml/min. The product was identified by comparison with the retention time of pure CH_3SCN (Fluorochem, Glossop, UK) and quantified by peak area. The structural identification of CH_3SCN produced by *Arabidopsis* was performed by gas chromatography/mass spectrometry (GC-MS; 5973 MSD, Agilent Technologies, Wilmington DE) using the HP-5ms semi-volatile column (30 m × 0.25 mm inner diameter, 0.25-μm film thickness, Agilent Technologies). The samples in 2.0-ml glass vials were

Downloaded from http://www.jbc.org/ at WILLAMETTE UNIVERSITY on August 29, 2014

incubated at 70 °C for 30 min, and each sampled 500-μl head space was injected into the column. The carrier gas (helium) flow was 0.9 ml/min. The column temperature was 30 °C, and the mass spectrometer was operated in electron impact mode at 70 eV. The CH_3SCN was identified by comparison with pure CH_3SCN in selected ion-monitoring mode at mass to charge ratios (*m*/*z*) of 73, 72, and 46 (supplemental Fig. S1).

Kinetic Analyses of Recombinant AtHOL Proteins—For kinetic analyses of AtHOL1, AtHOL2, and AtHOL3, glutathione *S*-transferase-tagged recombinant AtHOLs were expressed in *Escherichia coli* strain BL21, and tag-deleted AtHOLs were purified from soluble fractions as described (19). Each of the recombinant AtHOLs had 15 extra amino acids (GSTSLYKKAGSEFAL) at the N terminus. The assay mixture volume was 75 μl containing 0.1 M Tris acetate (pH 7.5), up to 1.58 μg of each of the AtHOLs, and varying concentrations of each substrate. *S*-(5′-Adenosyl)-L-methionine chloride (Wako, Osaka, Japan), KSCN (Nacalai Tesque, Kyoto, Japan), KCl (Nacalai Tesque), and $(NH_4)_2S$ (Nacalai Tesque) were used as substrates. Because the reaction rates were linear for at least 1 h (data not shown), all of the assay mixtures were incubated for 1 h at 25 °C. To stop the reaction, 1 M $HClO_4$ (75 μl) was added to the assay mixture. After centrifugation (16,100 × *g* for 10 min), 50 μl of the supernatant was injected into the HPLC system. The methyltransferase activities of AtHOLs were measured by quantifying the SAH produced by the enzymatic reactions.

Quantitative Analyses of NCS^- Synthesis in Arabidopsis—In the assay method that was established to sensitively and specifically quantify NCS^- in *Arabidopsis*, NCS^- was methylated by the recombinant AtHOL1 protein and converted to CH_3SCN, which was then quantified using GC-ECD.[3] The quantification was not influenced by ingredients in *Arabidopsis* extracts. To quantify NCS^- in homogenized *Arabidopsis*, ~4-week-old wild-type and T-DNA mutant lines were homogenized and centrifuged at 16,100 × *g* for 10 min. Each supernatant (20 μl) was analyzed. To investigate the effects of lower degrees of wounding on NCS^- synthesis, ~20 mg (fresh weight) of 4-week-old wild-type *Arabidopsis* seedlings were nicked by scissors along the mid-vein of all the leaves. Then the seedlings were homogenized on ice with 100 μl of 2.5% 5-sulfosalicylic acid to denature proteins contained in the samples, and the mixtures were neutralized by adding 0.2 N NaOH (100 μl). The homogenates were centrifuged at 16,100 × *g* for 10 min, and the supernatant (80 μl) was analyzed. Following the same procedure, basal level NCS^- concentration was determined with the intact *Arabidopsis* seedlings that were homogenized under denaturing conditions. To examine the influence of myrosinase on NCS^- production, 0.025 unit of myrosinase (thioglucosidase, EC 3.2.1.147; Sigma-Aldrich) was added to the extracts of the intact *Arabidopsis* seedlings.

Quantitative Analyses of CH_3SCN Synthesis in Arabidopsis—About 400 mg (fresh weight) of 4-week-old wild-type and T-DNA insertion mutant *Arabidopsis* were homogenized on ice. The samples were centrifuged at 16,100 × *g* for 10 min, and each supernatant (200 μl) was transferred to a 2.0-ml glass vial sealed with a screw cap fitted with a Teflon-lined septum and incubated overnight at 25 °C followed by the head-space analyses of CH_3SCN by GC-ECD. To examine the rate-limiting substrate in CH_3SCN production, the supernatants (180 μl) were mixed with 10 mM KSCN (20 μl) or 10 mM SAM (20 μl), incubated overnight, and analyzed by GC-ECD as indicated above. To examine the involvement of wounding in CH_3SCN production, 3-week-old wild-type *Arabidopsis* grown on soil were used. Wild-type *Arabidopsis* (~200 mg) was wounded as performed in the analyses of NCS^- synthesis indicated above. The samples were incubated overnight in 2.0-ml glass vials at 25 °C, and the 500-μl head space was analyzed for CH_3SCN by GC-ECD.

In Vitro Assay of Antibacterial Activity—Two bacterial pathogens, *Pseudomonas syringae* pv. *maculicola* (MAFF 302539) and *Erwinia carotovora* subsp. *carotovora* (MAFF 301879), which were obtained from the Genebank of the National Institute of Agrobiological Sciences, Japan, and a nonpathogenic bacterium, *E. coli* strain DH5α, were used for antibacterial activity assay. All of the bacteria were cultured in LB medium at 28 °C for *P. syringae* and *E. carotovora* and at 37 °C for *E. coli*. The bacteria were cultured overnight for *E. carotovora* and *E. coli* and for 2 days for *P. syringae*. The concentrations of KSCN and CH_3SCN causing 50% bacterial growth inhibition (IC_{50}) were determined by monitoring the cell populations at A_{600} (23, 24). The assay cultures (200 μl) were prepared from the bacterial suspension cultures at an A_{600} of 0.2, and KSCN and CH_3SCN were dissolved in water and ethanol, respectively. To avoid volatilization of CH_3SCN, each assay culture was incubated in a 2.0-ml glass vial sealed with a screw cap fitted with a Teflon-lined septum. The cultures were incubated at temperatures appropriate for each bacterium and cultured by shaking at 150 rpm for 15 h followed by measuring the A_{600}. The corresponding amounts of solvents used to dissolve KSCN and CH_3SCN did not affect bacterial growth (data not shown).

Pathogen Inoculation—*P. syringae* pv. *maculicola* was cultured in LB medium as described above and harvested by centrifugation at 4000 × *g* for 10 min. The bacterial pellet was rinsed once by 10 mM $MgCl_2$ and resuspended in 10 mM $MgCl_2$ at an A_{600} of 0.5 (25). The wild-type and *hol1 Arabidopsis* seeds (~400 seeds each) grown on half-strength MS agar medium were inoculated with droplets of the bacterial suspension (3 μl). For mock treatment, 10 mM $MgCl_2$ solution was used instead of the bacterial suspension. The survival rate of the seedlings grown for 19 days was evaluated based on the emergence of true leaves.

RESULTS

Phylogenetic Analysis of HOL Genes—BLAST searches of nucleotide sequence data bases were performed using the amino acid sequence of AtHOL1 as a query. Twenty-five HOL homologs from 19 different plant species were distributed from unicellular green algae to gymnosperms and angiosperms (supplemental Fig. S2). All of the plant species such as *Arabidopsis*, rice, poplar, wine grape, milo, moss (*Physcomitrella patens*), and red alga (*Cyanidioschyzon merolae*), for which the genomes have been completely sequenced, contained at least one HOL homolog, suggesting that HOL is a gene conserved in photo-

[3] Y. Nagatoshi and T. Nakamura, unpublished data.

Downloaded from http://www.jbc.org/ at WILLAMETTE UNIVERSITY on August 29, 2014

synthetic organisms. A phylogenetic tree was constructed based on the amino acid sequences of HOL homologs from multicellular species only (Fig. 1). The tree reflected the genealogy of the derived species. One of the most remarkable aspects was that HOL homologs from Brassicales plants including *Arabidopsis* were grouped into two clusters, cluster I and cluster II. However, HOL homologs from dicotyledonous plants other than Brassicales plants were all grouped in a single cluster, cluster III, and those from monocotyledonous plants were also all grouped in a single cluster, cluster IV. Because AtHOL1 and AtHOL2 formed a cluster together with TMT and MCT, we hypothesized that AtHOL proteins would have enzymatic activities similar to those of TMT and MCT. However, a detailed enzymatic characterization of the AtHOL proteins had yet to be reported.

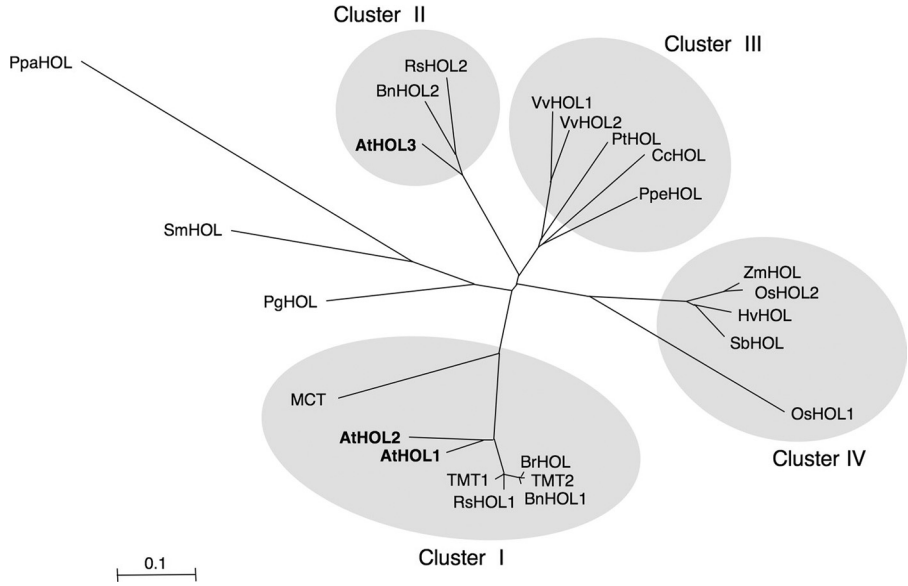

FIGURE 1. **Phylogenetic tree of HOL homologous proteins.** The amino acid sequences were aligned using the ClustalW program, and the phylogenetic tree was built using the Njplot program (unrooted). *Bar* = 0.1 amino acid substitutions/site. Sequences from *A. thaliana* (AtHOL1, AtHOL2, and AtHOL3: NM_129953, NM_129954, and NM_180072, respectively), *B. oleracea* (TMT1 and TMT2: AAK69760 and AAK69761, respectively), *Raphanus sativus* (EW721469 and ED955532 for RsHOL1; EW738453 for RsHOL2), *Brassica rapa* (BrHOL: ABL86248), *Brassica napus* (BnHOL1 and BnHOL2: TA24304_3708 and EV084135.1, respectively), *B. maritima* (MCT: AAD26120), *Vitis vinifera* (VvHOL1 and VvHOL2: GSVIVT00034750001 and GSVIVT00034749001, respectively), *Populus trichocarpa* (PtHOL: gw1.XVII.90.1), *Coffea canephora* (CcHOL: TA6982_49390), *Prunus persica* (PpeHOL: TA5314_3760), *Oryza sativa* (OsHOL1 and OsHOL2: NP_001051867 and NP_001056843, respectively), *Zea mays* (ZmHOL: TA188770_4577), *Hordeum vulgare* (HvHOL: TA43367_4513), *Sorghum bicolor* (SbHOL: Sb10g003780.1), *Picea glauca* (PgHOL: DR569353.1), *Selaginella moellendorfii* (SmHOL1: e_gw1.23.943.1), and *Physcomitrella patens* (PpaHOL: BY959091.1 and BY959091.1) were from the GenBank™ data base, the TIGR data base (www. tigr.org), and the U. S. Department of Energy Joint Genome Institute (www.jgi.doe.gov/).

Kinetic Characterization of Recombinant AtHOL Proteins—We first examined the substrate specificities and kinetic characteristics of the three AtHOL proteins. Among the compounds that worked as *in vitro* substrates for MCT or TMT (11, 14), three substrates (Cl^-, NCS^-, and HS^-) that were known to exist in *Arabidopsis* were analyzed. Glutathione *S*-transferase-tagged recombinant AtHOL proteins were expressed in *E. coli*, and tag-deleted AtHOL proteins were

TABLE 1

Kinetic parameters for methyltransferase activities of recombinant AtHOLs

ND, not detected. Data are the average of two technical repeats, and listed values represent S.E.

Variable substrate		Isoform	K_m	V_{max}	k_{cat}	k_{cat}/K_m
	(mM)		(mM)	(nmol s^{-1} mg $protein^{-1}$)	(s^{-1})	(s^{-1} mM^{-1})
KSCN[a]	1.6×10^{-2} - 2.5×10^{-1}	AtHOL1	$6.2 \times 10^{-2} \pm 1.2 \times 10^{-4}$	$2.2 \times 10^3 \pm 1.2 \times 10^2$	$5.8 \times 10^7 \pm 4.0 \times 10^6$	9.4×10^8
	1.3 - 20	AtHOL2	$1.8 \pm 4.9 \times 10^{-2}$	$2.6 \times 10^2 \pm 10$	$7.0 \times 10^6 \pm 2.7 \times 10^5$	3.8×10^6
	6.3 - 1.0×10^2	AtHOL3	$3.1 \pm 2.0 \times 10^{-1}$	$1.1 \times 10^2 \pm 21$	$3.0 \times 10^6 \pm 5.5 \times 10^5$	9.6×10^5
KCl[a]	78 - 1.3×10^3	AtHOL1	$2.8 \times 10^2 \pm 1.3 \times 10^2$	82 ± 7.6	$2.2 \times 10^6 \pm 2.0 \times 10^5$	7.9×10^3
	20 - 3.1×10^2	AtHOL2	$36 \pm 7.9 \times 10^{-2}$	$2.0 \times 10^2 \pm 12$	$5.4 \times 10^6 \pm 3.2 \times 10^5$	1.5×10^5
	78 - 1.3×10^3	AtHOL3	ND	ND	ND	ND
$(NH_4)_2S$[a]	1.1×10^{-1} - 1.7	AtHOL1	$2.6 \times 10^{-1} \pm 1.1 \times 10^{-1}$	$2.6 \times 10^3 \pm 2.2 \times 10^2$	$7.0 \times 10^7 \pm 5.8 \times 10^6$	2.7×10^8
	1.1×10^{-1} - 1.7	AtHOL2	$1.1 \pm 5.7 \times 10^{-2}$	$5.2 \times 10^2 \pm 17$	$1.4 \times 10^7 \pm 4.5 \times 10^5$	1.2×10^7
	1.1×10^{-1} - 1.7	AtHOL3	$1.3 \pm 1.7 \times 10^{-1}$	$1.3 \times 10^3 \pm 91$	$3.5 \times 10^7 \pm 2.4 \times 10^6$	2.8×10^7
SAM[b]	7.8×10^{-3} - 1.3×10^{-1}	AtHOL1	$9.2 \times 10^{-2} \pm 1.1 \times 10^{-4}$	$1.4 \times 10^3 \pm 70$	$3.6 \times 10^7 \pm 1.9 \times 10^6$	3.9×10^8
	7.8×10^{-3} - 1.3×10^{-1}	AtHOL2	$4.9 \times 10^{-2} \pm 2.1 \times 10^{-4}$	$2.0 \times 10^2 \pm 22$	$5.3 \times 10^6 \pm 6.0 \times 10^5$	1.1×10^8
	7.8×10^{-3} - 1.3×10^{-1}	AtHOL3	$4.0 \times 10^{-2} \pm 9.2 \times 10^{-5}$	$4.1 \times 10^2 \pm 20$	$1.1 \times 10^7 \pm 5.2 \times 10^5$	2.7×10^8

[a] Constant substrate was 0.5 mM SAM.
[b] Constant substrate was 1.7 mM $(NH_4)_2S$.

Downloaded from http://www.jbc.org/ at WILLAMETTE UNIVERSITY on August 29, 2014

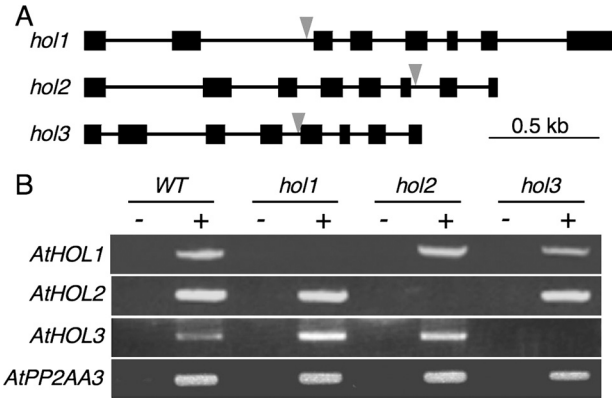

FIGURE 2. **T-DNA insertion *Arabidopsis* mutants of *AtHOL1*, *AtHOL2*, and *AtHOL3*.** *A*, schematic representation of the three *AtHOLs* with the T-DNA insertions in the mutants used in this study. *Black boxes* and *lines* represent exons and introns, respectively. *Gray arrows* represent locations of the T-DNA insertion. *B*, RT-PCR analysis of each *AtHOL* transcript in the wild type (*WT*) and the three mutant *Arabidopsis*. PCR templates were prepared with (+) or without (−) reverse transcriptase in cDNA synthesis reactions. PP2A was used as an internal control.

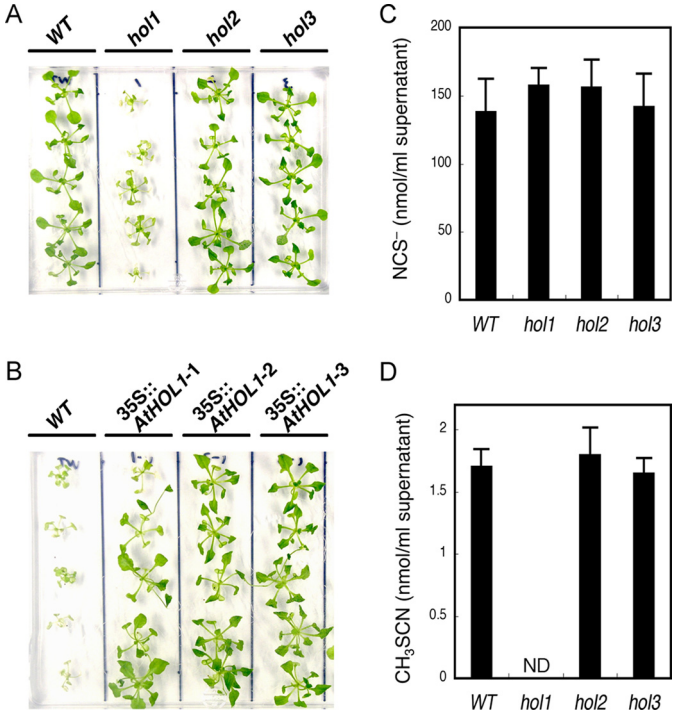

FIGURE 3. **Phenotypic analyses of *hol* mutants and *AtHOL1*-overexpressing *Arabidopsis*.** *A*, susceptibility of the wild type (*WT*) and the three *hol* mutant *Arabidopsis* to 1 mM KSCN. ~2 week-old seedlings grown on half-strength MS agar medium were transferred to medium containing 1 mM KSCN and grown for an additional 12 days. *B*, susceptibility of wild-type and *AtHOL1*-overexpressing *Arabidopsis* (35S::*AtHOL1*-1, 35S::*AtHOL1*-2, and 35S::*AtHOL1*-3) to 2.5 mM KSCN. ~4-week-old *AtHOL1*-overexpressing T2 seedlings were selected on half-strength MS agar medium containing 25 μg/ml kanamycin sulfate. Wild-type and screened *AtHOL1*-overexpressing seedlings were grown on half-strength MS agar medium containing 2.5 mM KSCN for 12 days. *C* and *D*, NCS^- (*C*) and CH_3SCN (*D*) synthesized in supernatants of the homogenized wild type and each *hol* mutant *Arabidopsis*. Four-week-old seedlings were analyzed. Data are the average of three technical repeats, and *bars* indicate S.E. *ND*, not detected. The NCS^- concentration was not significantly different ($p > 0.1$ by *t* test) among wild-type and the three mutant plants. The content of synthesized CH_3SCN was not significantly different ($p > 0.1$ by *t* test) among wild-type, *hol2* and *hol3* plants.

purified from soluble fractions (supplemental Fig. S3), which permitted more proper folding of the proteins than those prepared from insoluble fractions as done in previous studies (11, 13). Enzymatic activities for the three substrates were largely distinct among AtHOL isoforms (Table 1). The catalytic efficiencies (k_{cat}/K_m) of all AtHOL proteins for Cl^- (AtHOL1, 7.9×10^3; AtHOL2, 1.5×10^5; AtHOL3, not detected) were the lowest among the three analyzed substrates. On the other hand, AtHOL1 was highly reactive to NCS^- with a markedly high k_{cat}/K_m value (9.4×10^8). Based on the k_{cat}/K_m values, the most preferred substrate for both AtHOL2 and AtHOL3 was HS^-.

Isolation of AtHOL T-DNA Insertion Mutants—To investigate the physiological functions of the three *AtHOL* genes through *in vivo* experiments, we obtained T-DNA insertion *Arabidopsis* mutants for *AtHOL1*, *AtHOL2*, and *AtHOL3*. As shown in Fig. 2*A*, the mutants for *AtHOL1* (SALK_005204C), *AtHOL2* (SALK_021226C) and *AtHOL3* (SALK_014648C) possessed T-DNA inserts within introns 2, 6, and 4, respectively. Semiquantitative RT-PCR analyses with the obtained homozygous mutant plants, designated *hol1*, *hol2*, and *hol3*, indicated no transcript accumulation of the T-DNA-inserted *AtHOL* genes in each mutant (Fig. 2*B*). The obtained *hol1* plant was the same line used to show that *AtHOL1* is responsible for methyl halide production (18). There were no morphological defects in these mutant plants under normal growth conditions (data not shown).

Responses of Wild-type, AtHOL-disrupted, and AtHOL1-overexpressing Arabidopsis to NCS^-—Based on our prediction that the substrate preferences of AtHOLs shown in our kinetic analyses reflect the *in vivo* responses to the substrates, we examined the response of the wild type and the three *hol* mutant *Arabidopsis* toward NCS^-, HS^-, and Cl^-. All of the analyzed *Arabidopsis* seedlings showed the same growth under various concentrations of $(NH_4)_2S$ (as HS^-), NaCl (as Cl^-), and KCl (as Cl^-) (data not shown). On the other hand, among the three mutants, only *hol1* showed an increased sensitivity to 1 mM KSCN (as NCS^-) (Fig. 3*A*). *AtHOL1*-overexpressing *Arabidopsis* were grown on the medium containing a higher concentration of KSCN (2.5 mM), at which concentration the growth of wild-type *Arabidopsis* was inhibited (26, 27) (Fig. 3*B*). Compared with wild-type *Arabidopsis*, ~4-week-old *AtHOL1*-overexpressing plants showed clearer resistance to KSCN on the medium (Fig. 3*B*) than the seedlings just after germination (28). These results provided the first evidence that, among the three isoforms, only AtHOL1 metabolized NCS^- *in vivo*.

NCS^- and CH_3SCN Synthesis in Wild-type and AtHOL-disrupted Arabidopsis—Thereafter, we focused on the functional analyses of AtHOL1, which was highly reactive to NCS^-. To date, NCS^- has been detected in crushed glucosinolate-containing plants such as *Brassica* vegetables (16). Other reports showed that *in vitro* hydrolysis of indole glucosinolates by myrosinase produces NCS^- (16). However, to our knowledge, there have been no detailed *in vivo* studies demonstrating that NCS^- is derived solely from myrosinase-catalyzed hydrolysis of glucosinolates. Myrosinases and glucosinolates are stored separately in intact plant tissues. Upon tissue wounding, such as caused by chewing insects, these enzymes come into contact followed by glucosinolate hydrolysis (29–31). To investigate NCS^- synthesis, we first established an assay to sensitively and

Downloaded from http://www.jbc.org/ at WILLAMETTE UNIVERSITY on August 29, 2014

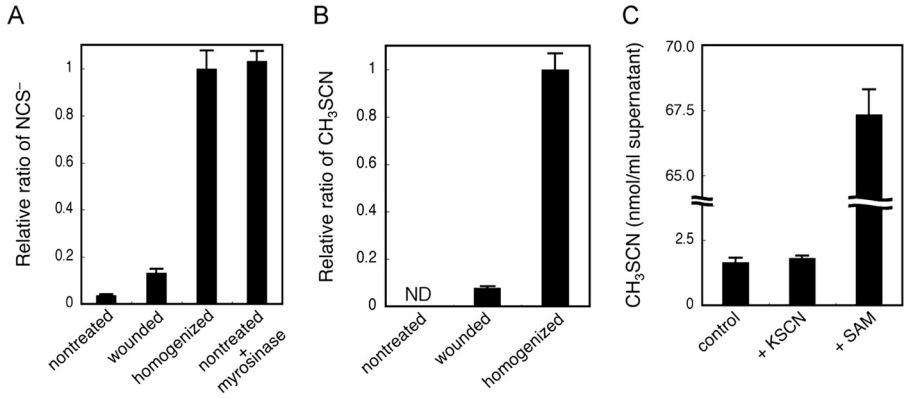

FIGURE 4. **Analysis of NCS^- and CH_3SCN synthesis in *Arabidopsis*.** *A*, role of wounding and myrosinase in NCS^- synthesis in wild-type *Arabidopsis*. The relative ratios of NCS^- accumulated in intact (*nontreated*), partially wounded (*wounded*), and thoroughly wounded (*homogenized*) *Arabidopsis* seedlings were examined. Purified myrosinase was added to the nontreated sample (*nontreated + myrosinase*). Data are the average of three to four technical repeats, and *bars* indicate S.E. The NCS^- concentration was significantly increased ($p < 0.001$ by *t* test) in wounded and homogenized samples compared with nontreated and wounded samples, respectively. The NCS^- concentration was not significantly different ($p > 0.1$ by *t* test) between homogenized and nontreated + myrosinase samples. *B*, role of wounding in CH_3SCN synthesis in wild-type *Arabidopsis*. The relative ratio of CH_3SCN synthesized in intact (*nontreated*), partially wounded (*wounded*), and thoroughly wounded (*homogenized*) *Arabidopsis* seedlings were examined. Data are the average of two technical repeats, and *bars* indicate S.E. ND means not detected. The content of synthesized CH_3SCN was significantly increased ($p < 0.003$ by *t* test) in homogenized samples compared with wounded samples. *C*, the rate-limiting substrate on CH_3SCN synthesis in *Arabidopsis*. CH_3SCN synthesis in the supernatants of the homogenized wild-type *Arabidopsis* (*control*) and the supernatants with 1 mM KSCN or with 1 mM SAM were determined. Data are the average of three technical repeats, and *bars* indicate S.E. The content of synthesized CH_3SCN was not significantly different ($p > 0.1$ by *t* test) between the control and +KSCN samples, and it was significantly increased ($p < 0.001$ by *t* test) in +SAM samples compared with the control.

specifically quantify NCS^- in the supernatant of homogenized, "thoroughly wounded" *Arabidopsis* seedlings. In the assay, NCS^- in the reaction mixture was converted to CH_3SCN by recombinant AtHOL1, which specifically methylates NCS^-, and then CH_3SCN was quantified by GC-ECD (see "Experimental Procedures"). By utilizing the established method, we demonstrated that NCS^- accumulated to ~140 μM in homogenized wild-type *Arabidopsis* seedlings, and the accumulation was unaffected by the disruption of each *AtHOL* gene (Fig. 3*C*). Because the concentration of accumulated NCS^- (ca. 140 μM) was much higher than the K_m value (62 μM) for NCS^- of the recombinant AtHOL1, we hypothesized that NCS^- was methylated to CH_3SCN by AtHOL1 in homogenized *Arabidopsis* seedlings. Indeed, GC-MS analyses confirmed the synthesis of CH_3SCN in the supernatant of homogenized wild-type *Arabidopsis* seedlings (supplemental Fig. S1). To investigate the involvement of the three *AtHOL* genes in CH_3SCN production, we quantified CH_3SCN synthesized in the supernatant of each homogenized *AtHOL*-disrupted mutant, *hol1*, *hol2*, and *hol3*. As a result, CH_3SCN synthesis in *hol1* was undetectable, whereas both *hol2* and *hol3* showed the same levels of CH_3SCN synthesis as wild-type *Arabidopsis* (Fig. 3*D*).

Involvement of Myrosinase in NCS^- and CH_3SCN Synthesis in Arabidopsis—We then verified the involvement of myrosinase in NCS^- and CH_3SCN production in *Arabidopsis*. The amount of NCS^- and CH_3SCN in the seedlings of leaves uniformly wounded by scissors was 13 and 7.7%, respectively, that of the homogenized ones (Fig. 4, *A* and *B*). In the unwounded seedlings, NCS^- accumulation was only 3.7% of the homogenized ones, and CH_3SCN synthesis was undetectable. These results suggested that both NCS^- and CH_3SCN synthesis varied based on the degree of wounding. When purified myrosinase was added to the assay mixture of unwounded seedlings, the NCS^- concentration increased to the same level as that in the homogenized seedlings. This result revealed that myrosinase was involved in the *in vivo* NCS^- production, and almost all of the accumulated NCS^- in homogenized *Arabidopsis* seedlings was actually derived from glucosinolates.

Rate-limiting Substrate for CH_3SCN Synthesis in Arabidopsis—We then determined the rate-limiting substrate for CH_3SCN synthesis. The addition of KSCN to the supernatant of homogenized *Arabidopsis* seedlings did not increase CH_3SCN synthesis, indicating that all the SAM was exhausted in the supernatant. Meanwhile the addition of SAM increased the synthesis by ~40-fold (Fig. 4*C*). These results indicated that the supply of SAM may be rate-limiting for CH_3SCN synthesis, although CH_3SCN synthesis was triggered by wounding that first induced NCS^- synthesis.

In Vitro Antibacterial Activities of NCS^- and CH_3SCN—Thus far, there have been several studies reporting on the biological activities of glucosinolate-hydrolyzed products, typically isothiocyanates and nitriles (29). As for NCS^-, none of the reported studies could detect biological activities on the analyzed bacteria and fungi (15, 32). On the other hand, a limited number of studies have demonstrated that bacteria belonging to *Pseudomonas* genus showed a negative chemotaxis to CH_3SCN (33, 34). Based on this finding, we hypothesized that CH_3SCN synthesized by *Arabidopsis* also had biological activities toward bacteria. To answer this question, we examined the influence of CH_3SCN on bacterial growth. *P. syringae* pv. *maculicola* and *E. carotovora* subsp. *carotovora*, which are pathogenic to *Arabidopsis* and normally invade the wound site, and non-pathogenic *E. coli* strain DH5α were selected, and their growth was investigated under various concentrations of KSCN and CH_3SCN. The KSCN concentration that caused 50% inhibition of bacterial growth (IC_{50}) was over 50 mM for all of the bacteria analyzed (Fig. 5). On the other hand, the IC_{50} of CH_3SCN for *P. syringae* pv. *maculicola*, *E. carotovora* subsp. *carotovora*, and *E. coli* was dramatically lowered to 1.2, 9.4, and 3.6 mM, respectively. These results suggested, for the first time, that the conversion of NCS^- into CH_3SCN catalyzed by AtHOL1 increased the toxicity of NCS^- to the bacteria.

Enhanced Susceptibility of AtHOL1-disrupted Arabidopsis to P. syringae pv. maculicola—To investigate whether the pathogens were affected by CH_3SCN synthesis *in planta*, we tested the wild-type and *hol1 Arabidopsis* on their susceptibility to *P. syringae* pv. *maculicola*. Because younger wild-type seedlings accumulate larger amounts of *AtHOL1* mRNA than 4-week-old seedlings (18), we hypothesized that the differences in suscep-

Downloaded from http://www.jbc.org/ at WILLAMETTE UNIVERSITY on August 29, 2014

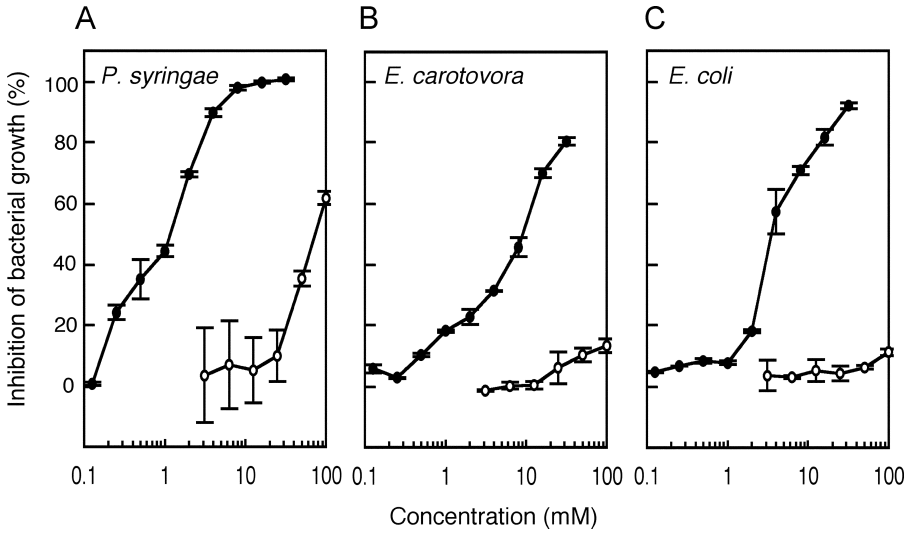

FIGURE 5. ***In vitro* antibacterial activity of KSCN and CH_3SCN.** Growth inhibition of the plant bacterial pathogens *P. syringae* pv. *maculicola* (*A*) and *E. carotovora* subsp. *carotovora* (*B*) and a non-pathogenic bacterium, *E. coli* strain DH5α (*C*), were measured at varying concentrations of KSCN (*open circles*) and CH_3SCN (*filled circles*). The ratio of growth inhibition was recorded after 15 h. Data are the average of two technical repeats, and *bars* indicate S.E.

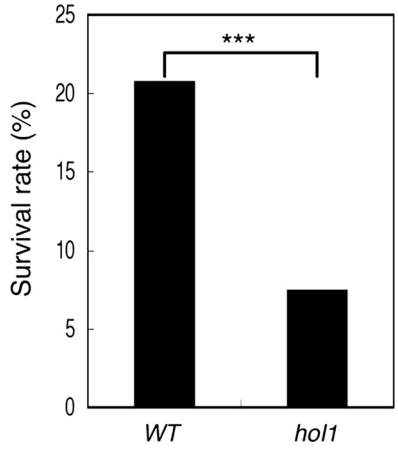

FIGURE 6. **Susceptibility of wild-type and *AtHOL1*-disrupted *Arabidopsis* toward *P. syringae* pv. *maculicola*.** The survival rate of the seedlings was evaluated based on the emergence of true leaves and was normalized by the seed germination rate of wild-type (*WT*) and *hol1 Arabidopsis*. The germination rate between wild-type and *hol1* seeds was not significantly different (data not shown). The survival rate was significantly different (***, $p < 0.001$, $\chi^2 = 31.79$ by chi-square test) between wild-type ($n = 452$) and *hol1* ($n = 428$) *Arabidopsis*. The data are derived from three independent experiments for both seeds.

tibility between wild-type and *hol1 Arabidopsis* might be observed with younger seedlings. Seeds of wild-type and *hol1 Arabidopsis* were infected with *P. syringae* pv. *maculicola* and grown for 19 days on half-strength MS agar medium (supplemental Fig. S4). Indeed, the percentage of surviving seedlings was significantly lower for *hol1* (7.5%) compared with wild-type *Arabidopsis* (21%) (Fig. 6), suggesting that *hol1 Arabidopsis* increased the susceptibility toward *P. syringae* pv. *maculicola.*

DISCUSSION

AtHOL1 Was Highly Reactive to NCS^- rather than Cl^- in Arabidopsis—We demonstrated, for the first time, the comparative kinetic analyses of all the HOL isoforms in a single plant species and found that AtHOL1 was highly reactive to NCS^-. AtHOL1 was originally reported to be involved in the production of methyl halides in *Arabidopsis* (18). However, the kinetic analyses of recombinant AtHOL1 showed that the k_{cat}/K_m value for Cl^- was lowest among the analyzed substrates, and the K_m value (280 mM) was much higher than the normal intracellular Cl^- concentration (Table 1). The activity of AtHOL3 for Cl^- was undetectable, whereas that of AtHOL2 was the highest among the three isoforms. However, the contribution of AtHOL2 to CH_3Cl production was hypothesized to be subtle because methyl halide emissions depend mostly on *AtHOL1* (18), and *AtHOL2* mRNA accumulation is much lower than *AtHOL1* (19). Ni and Hager (11) proposed that the physiological function of MCT, an AtHOL1 homolog in a Brassicales plant, is to regulate the intracellular Cl^- concentration. However, the amount of CH_3Cl emitted from *Arabidopsis* was so low that intracellular Cl^- concentrations could not be reduced in *Arabidopsis* tissues. This hypothesis is supported by the results of our kinetic analyses showing the lower activities of AtHOLs toward Cl^- and by the results showing that none of the *hol* mutants was more sensitive than wild-type *Arabidopsis* toward 0–100 mM KCl or NaCl in the half-strength MS agar medium (data not shown). These results together suggest that Cl^- is not the physiological substrate for AtHOL proteins.

HS^- was the most preferred substrate for AtHOL2 and AtHOL3 and the second most preferred substrate for AtHOL1 among the analyzed substrates. Therefore, the activity of AtHOL proteins for HS^- may also contribute to the synthesis of CH_3SH (35, 36), which is reported also to be synthesized from methionine hydrolysis by methionine γ-lyase in *Arabidopsis* (37).

On the other hand, NCS^- was highly reactive for AtHOL1 with a k_{cat}/K_m that was ~250- and 980-fold higher than that for AtHOL2 and AtHOL3, respectively. The NCS^- concentration (~140 μM) in the homogenized *Arabidopsis* tissue was higher than the K_m value (62 μM) of AtHOL1 for NCS^- (Table 1). Furthermore, CH_3SCN synthesis was dependent on AtHOL1 (Fig. 3). These results suggest that NCS^- is the physiological substrate for AtHOL1. Through reverse genetic and biochemical analyses, we have demonstrated that AtHOL1 is responsible for CH_3SCN production *in vivo* (Fig. 3).

NCS^- Was Derived from Glucosinolate Hydrolysis in Arabidopsis—We demonstrated that NCS^- and CH_3SCN synthesis varied based on the degree of wounding; the synthesis of almost all NCS^- was derived from glucosinolates through hydrolysis by myrosinase (Fig. 4). Our *in vivo* studies demonstrated a novel metabolic pathway of a glucosinolate breakdown product catalyzed by AtHOL1. Indole glucosinolate breakdown products have also been detected on intact leaf surfaces (38). Glucosinolates in intact tissues of *Arabidopsis*

Downloaded from http://www.jbc.org/ at WILLAMETTE UNIVERSITY on August 29, 2014

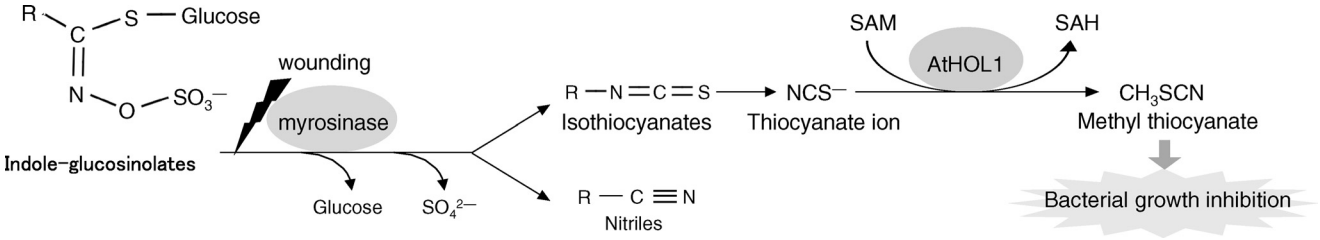

FIGURE 7. **Proposed model of AtHOL1 function based on the results demonstrated in this study.**

are constantly renewed in the cell (39, 40). Sulfur deficiency also induces a conditional turnover of glucosinolates in *Arabidopsis* (41). Hence the basal level of NCS^- in *Arabidopsis* tissues observed in Fig. 4*A* was possibly derived from the turnover of glucosinolates.

Role of CH_3SCN Production in Plant Defense—Only about 1% of NCS^- could be converted to CH_3SCN, possibly because of the exhaustion of SAM in the supernatant of homogenized *Arabidopsis* seedlings (Fig. 3, *C* and *D*). Thus, the primary physiological role of AtHOL1 may not be the detoxification of NCS^- by volatilization (14). Rather, CH_3SCN synthesis (by methylation of NCS^-) markedly increased its toxicity toward the bacteria (Fig. 5). To date, the biological activities of glucosinolate breakdown products such as nitriles and isothiocyanates have been studied in detail (29). For example, isothiocyanates contain antibacterial activities (15), and indole-3-acetonitrile has antifungal activity (42). Indole-3-carbinol and indole-3-acetonitrile act as a stimulant and a deterrent, respectively, for an ovipositing butterfly (38). CH_3SCN reported herein may be considered a novel member of such biologically active compounds derived from glucosinolates. Although further studies are needed to understand how CH_3SCN inhibits bacterial growth, CH_3SCN indeed showed an inhibitory effect on the analyzed bacteria ranging from plant pathogens to a bacterium unrelated to plant pathogens. The observed effect on the different classes of bacteria implies that CH_3SCN synthesis is involved in a broad spectrum antibacterial defense in *Arabidopsis*. Indeed, our *in vivo* studies have demonstrated that the disruption of *AtHOL1* increases the susceptibility of the mutant seedlings toward *P. syringae* pv. *maculicola* (Fig. 6). These results imply that CH_3SCN synthesis catalyzed by AtHOL1 is at least in part responsible for the resistance to *P. syringae* pv. *maculicola*.

To date, indole glucosinolates are the only glucosinolates reported to generate NCS^- through a myrosinase-catalyzed hydrolysis that also exists in *Arabidopsis*. Indole glucosinolate synthesis is induced by methyl jasmonate (43), elicitors derived from the bacterial pathogen *E. carotovora* (32), and the fungal pathogen *Alternaria brassicae* (44) and by an interaction with a mycorrhizal fungus (45). *PEN2* in *Arabidopsis* is responsible for efficient entry by the non-host fungus *Blumeria graminis* f. sp. *hordei* (46). PEN2 may preferentially hydrolyze indole glucosinolates producing defensive compounds at incipient fungal entry sites without tissue damage (40, 46). These studies (40, 42–46) imply that CH_3SCN production by AtHOL1 might also be induced by pathogens, in which case NCS^- synthesis and a continuous supply of SAM within an intact cell would cause a higher level of CH_3SCN synthesis at the pathogen entry site. These observations may explain the difference between the CH_3SCN concentration in homogenized wild-type *Arabidopsis* (Fig. 3*D*) and the CH_3SCN concentration that inhibited bacterial growth (Fig. 5).

Methyl Halide Production by AtHOL1—In conclusion, our study suggests that AtHOL1 metabolizes glucosinolate-derived NCS^-, which induces the plant defense mechanism (CH_3SCN synthesis) (Fig. 7). Hence, methyl halide production by AtHOL1 could be considered a byproduct of NCS^- metabolism in *Arabidopsis*. Glucosinolate-containing plants generally show a high level of methyl halide synthesis (47), which might be due to *HOL* genes belonging to cluster I (Fig. 1). On the other hand, we have shown that HOL homologs are widespread among photosynthetic organisms (Fig. 1). Hence, HOL homologs not found in cluster I may function differently than AtHOL1 and function commonly in photosynthetic organisms. Further analyses are needed to elucidate whether there is a common function for HOL homologs and their involvement in methyl halide emission, which is an important issue in global atmospheric chemistry.

Acknowledgments—We thank the Nottingham Arabidopsis Stock Centre for the SALK T-DNA lines and the Genebank of the National Institute of Agrobiological Sciences, Japan, for the plant pathogens.

REFERENCES

1. World Meteorological Organization (2007) *Scientific Assessment of Ozone Depletion: 2006, Global Ozone Research and Monitoring Project-Report 50*, World Meteorological Organization, Geneva
2. Khalil, M. A., Moore, R. M., Harper, D. B., Lobert, J. M., Erickson, D. J., Koropalov, V., Sturges, W. T., and Keene, W. C. (1999) *J. Geophys. Res.* **104,** 8333–8346
3. Lobert, J. M., Keene, W. C., Logan, J. A., and Yevich, R. (1999) *J. Geophys. Res.* **104,** 8373–8390
4. Rhew, R. C., Miller, B. R., Bill, M., Goldstein, A. H., and Weiss, R. F. (2002) *Biogeochemistry* **60,** 141–161
5. Saito, T., and Yokouchi, Y. (2006) *Atmos. Environ.* **40,** 2806–2811
6. Harper, D. B., Hamilton, J. T., Ducrocq, V., Kennedy, J. T., Downey, A., and Kalin, R. M. (2003) *Chemosphere* **52,** 433–436
7. Yokouchi, Y., Ikeda, M., Inuzuka, Y., and Yukawa, T. (2002) *Nature* **416,** 163–165
8. Saito, T., and Yokouchi, Y. (2008) *Geophys. Res. Lett.* **35,** in press
9. Wuosmaa, A. M., and Hager, L. P. (1990) *Science* **249,** 160–162
10. Ni, X., and Hager, L. P. (1998) *Proc. Natl. Acad. Sci. U.S.A.* **95,** 12866–12871
11. Ni, X., and Hager, L. P. (1999) *Proc. Natl. Acad. Sci. U.S.A.* **96,** 3611–3615
12. Attieh, J. M., Hanson, A. D., and Saini, H. S. (1995) *J. Biol. Chem.* **270,** 9250–9257
13. Attieh, J., Djiana, R., Koonjul, P., Etienne, C., Sparace, S. A., and Saini, H. S. (2002) *Plant Mol. Biol.* **50,** 511–521
14. Attieh, J., Kleppinger-Sparace, K. F., Nunes, C., Sparace, S. A., and Saini,

Downloaded from http://www.jbc.org/ at WILLAMETTE UNIVERSITY on August 29, 2014

H. S. (2000) *Plant Cell Environ.* **23,** 165–174
15. Brown, J., and Morra, M. J. (2005) *Glucosinolate-containing Seed Meal as a Soil Amendment to Control Plant Pests, 2000–2002*, University of Idaho, Moscow, ID
16. Agerbirk, N., Olsen, C. E., and Sorensen, H. (1998) *J. Agric. Food Chem.* **46,** 1563–1571
17. Agerbirk, N., De Vos, M., Kim, J., and Jander, G. (2008) *Phytochem. Rev.* **8,** 101–120
18. Rhew, R. C., Østergaard, L., Saltzman, E. S., and Yanofsky, M. F. (2003) *Curr. Biol.* **13,** 1809–1813
19. Nagatoshi, Y., and Nakamura, T. (2007) *Plant Biotechnol.* **24,** 503–506
20. Czechowski, T., Stitt, M., Altmann, T., Udvardi, M. K., and Scheible, W. R. (2005) *Plant Physiol.* **139,** 5–17
21. Thompson, J. D., Higgins, D. G., and Gibson, T. J. (1994) *Nucleic Acids Res.* **22,** 4673–4680
22. Perrière, G., and Gouy, M. (1996) *Biochimie* **78,** 364–369
23. Feder, R., Dagan, A., and Mor, A. (2000) *J. Biol. Chem.* **275,** 4230–4238
24. Cammue, B. P., De Bolle, M. F., Terras, F. R., Proost, P., Van Damme, J., Rees, S. B., Vanderleyden, J., and Broekaert, W. F. (1992) *J. Biol. Chem.* **267,** 2228–2233
25. Kabisch, U., Landgraf, A., Krause, J., Bonas, U., and Boch, J. (2005) *Microbiology* **151,** 269–280
26. Stiehl, B., and Bible, B. B. (1989) *HortScience* **24,** 99–101
27. Ju, H. Y., Bible, B. B., and Chong, C. (1983) *J. Chem. Ecol.* **9,** 1255–1262
28. Midorikawa, K., Nagatoshi, Y., and Nakamura, T. (2009) *Plant Biotechnol.* **26,** in press
29. Wittstock, U., and Halkier, B. A. (2002) *Trends Plant Sci.* **7,** 263–270
30. Bones, A. M., and Rossiter, J. T. (2006) *Phytochemistry* **67,** 1053–1067
31. Grubb, C. D., and Abel, S. (2006) *Trends Plant Sci.* **11,** 89–100
32. Brader, G., Tas, E., and Palva, E. T. (2001) *Plant Physiol.* **126,** 849–860
33. Ohga, T., Masduki, A., Kato, J., and Ohtake, H. (1993) *FEMS Microbiol. Lett.* **113,** 63–66
34. Masduki, A., Nakamura, J., Ohga, T., Umezaki, R., Kato, J., and Ohtake, H. (1995) *J. Bacteriol.* **177,** 948–952
35. Bates, T. S., Lamb, B. K., Guenther, A., Dignon, J., and Stoiber, R. E. (1992) *J. Atmos. Chem.* **14,** 315–337
36. Bentley, R., and Chasteen, T. G. (2004) *Chemosphere* **55,** 291–317
37. Goyer, A., Collakova, E., Shachar-Hill, Y., and Hanson, A. D. (2007) *Plant Cell Physiol.* **48,** 232–242
38. De Vos, M., Kriksunov, K. L., and Jander, G. (2008) *Plant Physiol.* **146,** 916–926
39. Petersen, B. L., Chen, S., Hansen, C. H., Olsen, C. E., and Halkier, B. A. (2002) *Planta* **214,** 562–571
40. Bednarek, P., Pislewska-Bednarek, M., Svatos, A., Schneider, B., Doubsky, J., Mansurova, M., Humphry, M., Consonni, C., Panstruga, R., Sanchez-Vallet, A., Molina, A., and Schulze-Lefert, P. (2009) *Science* **323,** 101–106
41. Hirai, M. Y., Yano, M., Goodenowe, D. B., Kanaya, S., Kimura, T., Awazuhara, M., Arita, M., Fujiwara, T., and Saito, K. (2004) *Proc. Natl. Acad. Sci. U.S.A.* **101,** 10205–10210
42. Pedras, M. S., Nycholat, C. M., Montaut, S., Xu, Y., and Khan, A. Q. (2002) *Phytochemistry* **59,** 611–625
43. Sasaki-Sekimoto, Y., Taki, N., Obayashi, T., Aono, M., Matsumoto, F., Sakurai, N., Suzuki, H., Hirai, M. Y., Noji, M., Saito, K., Masuda, T., Takamiya, K., Shibata, D., and Ohta, H. (2005) *Plant J.* **44,** 653–668
44. Doughty, K. J., Porter, A. J. R., Morton, A. M., Kiddle, G., Bock, C. H., and Wallsgrove, R. (1991) *Ann. Appl. Biol.* **118,** 469–477
45. Rostás, M., Bennett, R., and Hilke, M. (2002) *J. Chem. Ecol.* **28,** 2449–2463
46. Lipka, V., Dittgen, J., Bednarek, P., Bhat, R., Wiermer, M., Stein, M., Landtag, J., Brandt, W., Rosahl, S., Scheel, D., Llorente, F., Molina, A., Parker, J., Somerville, S., and Schulze-Lefert, P. (2005) *Science* **310,** 1180–1183
47. Saini, H. S., Attieh, J. M., and Hanson, A. D. (1995) *Plant Cell Environ.* **18,** 1027–1033

Downloaded from http://www.jbc.org/ at WILLAMETTE UNIVERSITY on August 29, 2014